PROCEEDINGS OF SCIENCE

Gauge independence of Abelian confinement mechansim in SU2 gluodynamics

Tsuneo Suzuki[*ab†], **Katsuya Ishiguro,**[ab], **Yoshiaki Koma,**[c], **Toru Sekido,**[ab]

[a] *Institute for Theoretical Physics, Kanazawa University, Kanazawa 920-1192, Japan*
[b] *RIKEN, Radiation Laboratory, Wako 351-0158, Japan*
[c] *Numazu College of Technology, Numazu 410-8501, Japan*
E-mail:
suzuki@hep.s.kanazawa-u.ac.jp,
ishiguro@hep.s.kanazawa-u.ac.jp,
koma@rcnp.osaka-u.ac.jp,
toryu@hep.s.kanazawa-u.ac.jp

Abelian mechanism of non-Abelian color confinement is observed in a gauge-independent way by high precision lattice Monte Carlo simulations in gluodynamics. An Abelian gauge field is extracted with no gauge-fixing. A static quark-antiquark potential derived from Abelian Polyakov loop correlators gives us the same string tension as the non-Abelian one. The Hodge decomposition of the Abelian Polyakov loop correlator to the regular photon and the singular monopole parts also reveals that only the monopole part is responsible for the string tension. The investigation of the flux-tube profile then shows that Abelian electric fields defined in an arbitrary color direction are squeezed by monopole supercurrents with the same color direction, and the quantitative features of flux squeezing are consistent with those observed previously after Abelian projections with gauge fixing. Gauge independence of Abelian and monopole dominance strongly supports that the mechanism of non-Abelian color confinement is due to the Abelian dual Meissner effect.

The XXV International Symposium on Lattice Field Theory
July 30-4 August 2007
Regensburg, Germany

[*] Speaker.
[†] The authors would like to thank RIKEN, RCNP and YITP for their support of computer facilities.

PoS(LATTICE 2007)335

1. Introduction and summary

Color confinement in quantum chromodynamics (QCD) is still an important unsolved problem. 't Hooft [1] and Mandelstam [2] conjectured that the QCD vacuum is a kind of a magnetic superconducting state caused by condensation of magnetic monopoles and an effect dual to the Meissner effect works to confine color charges. However, to find color magnetic monopoles which condense is not straightforward in QCD.

An interesting idea to realize this conjecture is to project SU(3) QCD to an Abelian $[U(1)]^2$ theory by a partial gauge fixing [3]. Then color magnetic monopoles appear as a topological object. Condensation of the monopoles causes the dual Meissner effect [4, 5, 6]. However there are infinite ways of the above partial gauge-fixing and whether the 't Hooft scheme is gauge independent or not is not clear. Moreover why non-Abelian color charges are confined in the framework of the Abelian mechanism is not clarified.

Numerically, an Abelian projection in non-local gauges such as the maximally Abelian (MA) gauge [7, 8] has been found to support the Abelian confinement scenario beautifully [9, 10]. Very recently, the present authors have shown that the Abelian dominance and the dual Meissner effect are observed clearly also in local unitary gauges such as $F12$ and Polyakov (PL) gauges [11]. These results strongly suggest that the Abelian confinement mechanism is gauge-independent.

Here we study the QCD vacuum after extracting an Abelian link field in a completely gauge-independent way without adopting any special local or non-local gauge fixing. We observe that an Abelian confinement mechanism due to condensation of monopoles is realized. A static potential derived from Abelian Polyakov loop correlators gives us the correct string tension. Moreover only the monopole part in the Abelian Polyakov loop is responsible for the string tension. Abelian electric fields defined in an arbitrary color direction are squeezed and the corresponding monopole currents play the role of magnetic supercurrents. States which are neutral in all color directions are not confined and appear as a physical state. It is just a color-singlet state. Hence, confinement of non-Abelian color charges, not that of Abelian charges, is explained in the framework of the gauge-independent Abelian mechanism.

2. Abelian dominance

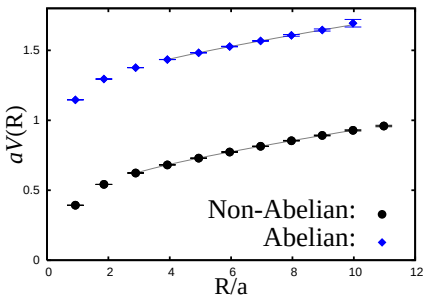

Figure 1: The Abelian static potential in comparison with the non-Abelian one. The solid lines denote the best fit to a function $V_{\rm fit}$.

Firstly we discuss an Abelian static potential. We generate thermalized gluon configurations using the Wilson action at a coupling constant $\beta = 2.5$ on the lattice $N^4 = 24^4$, where the lattice spacing $a(\beta) = .0836(8)$ [fm]. For simplicity we consider SU(2) gluodynamics, since essential features are not altered in SU(3). We extract a 2×2 diagonal Abelian link field in an arbitrary color direction. For example, in the σ_3 direction,

$$U_\mu(s) = U^0_\mu(s) + i\vec{\sigma}\vec{U}_\mu(s) = C_\mu(s)\cdot\mathrm{diag}\left[e^{i\theta_\mu(s)}, e^{-i\theta_\mu(s)}\right],$$

where $\theta_\mu(s) = \arctan(U^3_\mu(s)/U^0_\mu(s))$. Note that we can do the same also in the σ_1 or σ_2 direction, since all three components are equivalent with no gauge-fixing. By using the multi-level noise reduction method [12], we evaluate the Abelian static potential from the correlation function of the Abelian Polyakov loop operator

$$P_A = \exp[i\sum_{k=0}^{N-1}\theta_4(s+k\hat{4})]\,, \tag{2.1}$$

separated at a distance R. For the multi-level method, the number of sublattices adopted is 6 and the sublattice size is 4. The results are surprisingly beautiful as seen from Fig. 1. To reduce the lattice artifact due to finite-lattice cutoff, we plot the potential using $O(a^2)$ improved distances [13, 14]. We try to fit the data to a usual function $V_{\rm fit} = \sigma R - c/R + \mu$ and find almost the same string tension and the Coulombic coefficient as shown in Table 1, indicating Abelian dominance. Here the number of independent vacuum configurations is 10 in all cases. The errors are determined by the jackknife method. Our results of the string tension are consistent with theoretical observations on the basis of reasonable assumptions [15, 16].

Table 1: Best fitted values of the string tension $a^2\sigma$, the Coulombic coefficient c and the constant $a\mu$. NA and A-NGF denote Non-Abelian and Abelian with no gauge-fixing. $N_{\rm iup}$ is the number of internal updates in the multi-level method. FR means the fitting range. The χ^2 for the central value is $\chi^2/N_{df} < 0.1$.

	σa^2	c	μa	FR(R/a)	$N_{\rm iup}$
NA	0.0348(7)	0.243(6)	0.607(4)	3.92 - 9.97	15000
A-NGF	0.0352(16)	0.231(39)	1.357(17)	4.94 - 9.97	160000

3. Monopole dominance

Secondly we discuss the role of monopole contribution. The monopole part of the operator can be extracted as follows. The Abelian Polyakov loop (2.1) can be written by a product of a photon and a Dirac-string parts [17]. Note that

$$\theta_4(s) = -\sum_{s'} D(s-s')[\partial'_\nu\theta_{\nu 4}(s') + \partial_4(\partial'_\nu\theta_\nu(s'))]\,, \tag{3.1}$$

where $D(s-s')$ is the lattice Coulomb propagator, $\theta_{\mu\nu}(s) = \partial_\mu\theta_\nu(s) - \partial_\nu\theta_\mu(s)$ and $\partial_\nu(\partial'_\nu)$ is a forward(backward) difference. We have used $\partial_\nu\partial'_\nu D(s-s') = -\delta_{ss'}$. The second term in the right-hand side of (3.1) does not contribute to the Abelian Polyakov loop (2.1). Now $\theta_{\mu\nu}(s) = \bar{\theta}_{\mu\nu}(s) +$

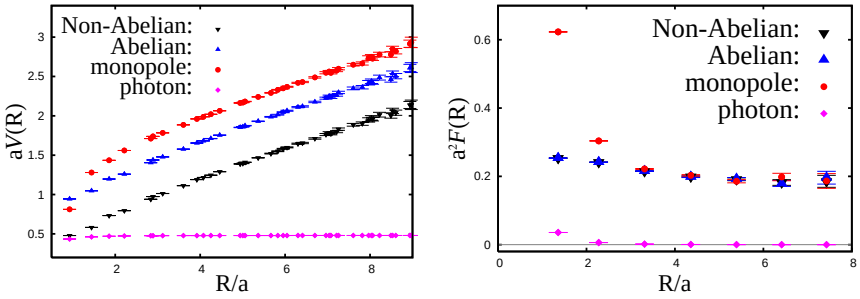

Figure 2: The static potential (left) and the force (right) from the Abelian (P_A), the monopole (P_{mon}) and the photon contributions (P_{ph}) in comparison with the non-Abelian ones.

Table 2: Best fitted values of the string tension σa^2 and the Coulomb coefficient c. M-NGF (P-NGF) denotes the monopole (the photon) part.

	σa^2	c	μa	FR(R/a)	χ^2/N_{df}
NA	0.181(8)	0.25(15)	0.54(7)	3.92 - 8.50	1.00
A-NGF	0.183(8)	0.20(15)	0.98(7)	3.92 - 8.23	1.00
M-NGF	0.183(6)	0.25(11)	1.31(5)	3.92 - 6.71	0.98
P-NGF	-0.0002(1)	0.010(1)	0.48(1)	4.94 - 9.44	1.02

$2\pi n_{\mu\nu}(s)$ $(|\bar{\theta}_{\mu\nu}| < \pi)$, where $n_{\mu\nu}(s)$ is an integer corresponding to the number of the Dirac string. Hence we obtain $P_A = P_{ph} \cdot P_{mon}$, where

$$P_{ph} = \exp\{-i \sum_{k=0}^{N-1} \sum_{s'} D(s+k\hat{4}-s')\partial'_\nu \bar{\theta}_{\nu 4}(s')\},$$
$$P_{mon} = \exp\{-2\pi i \sum_{k=0}^{N-1} \sum_{s'} D(s+k\hat{4}-s')\partial'_\nu n_{\nu 4}(s')\}.$$

We call P_{ph} and P_{mon} the photon and the monopole contributions, respectively, since the Dirac string $n_{\beta\gamma}(s)$ leads us to a monopole current $k_\mu(s) = (1/2)\varepsilon_{\mu\alpha\beta\gamma}\partial_\alpha n_{\beta\gamma}(s+\hat{\mu})$ [18].

We need a non-local Coulomb propagator in the separation, so that the multi-level noise reduction method cannot be applied in this case. Here we consider a $T \neq 0$ system in the confinement phase with the Wilson action on $24^3 \times 4$ lattice. We use about 6000 thermalized configurations at $\beta = 2.2$, where the lattice spacing is $a(\beta) = .191(8)$ [fm]. Since the expectation values of the correlation functions of P_A, P_{ph} and P_{mon} are still very small with no gauge-fixing, we adopt a new noise reduction method. For a thermalized vacuum ensemble, we produce many gauge copies applying random gauge transformations, compute the operator for each copy, and take the average of all copies. Note that as long as a gauge-invariant operator is evaluated, such copies are identical, but they are not if a gauge-variant operator is evaluated. Practically, we prepare 1000 gauge copies for each configuration. We also apply one-step hypercubic blocking (HYP) [19] to the temporal links for further noise reduction.

We obtain very good signals for the Abelian, the monopole and the photon contributions to

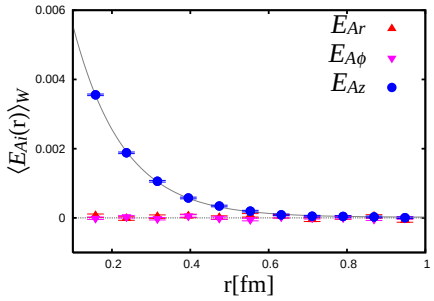

Figure 3: The profile of the Abelian electric fields for $W(R=5a,T=5a)$.

the static potential as shown in Fig. 2. We try to fit the potential in Fig. 2 to the function $V_{\rm fit}$ and extract the string tension and the Coulombic coefficient of each potential as summarized in Table 2. Abelian dominance is seen again beautifully in this case. Moreover, we can see monopole dominance, namely, only the monopole part of the Polyakov loop correlator is responsible for the string tension. The photon part has no linear potential. The agreement among the string tensions coming from non-Abelian, Abelian and monopole Polyakov loop correlators is almost perfect as seen also from the force in Fig. 2 in comparison with the MA case, where only 80-90 percent agreement is observed at finite lattice spacings. The short-range behavior of the potential may be affected by HYP.

4. Abelian dual Meissner effect

Thirdly we discuss the Abelian dual Meissner effect. We investigate the Abelian flux-tube profile by evaluating connected correlation functions [20, 21] between a Wilson loop W and Abelian operators $\mathscr{O}_A$ constructed by Abelian link fields,

$$\langle \mathscr{O}_A(r)\rangle_W = \frac{\langle {\rm Tr}\left[LW(r=0,R,T)L^\dagger \sigma^3 \mathscr{O}_A(r)\right]\rangle}{\langle {\rm Tr}\left[W(R,T)\right]\rangle},$$

where L is a product of non-Abelian link fields (a Schwinger line) connecting the Wilson loop with the Abelian operator. We may use the cylindrical coordinate (r,ϕ,z) to parametrize the the q-$\bar{q}$ system, where the z axis corresponds to the q-$\bar{q}$ axis and r to the transverse distance. We are interested in the field profile as a function of r on the mid-plane of the q-$\bar{q}$ distance. In this calculation, we employ the improved Iwasaki gauge action [22] with the coupling constant $\beta = 1.20$, which corresponds to the lattice spacing $a(\beta) = .0792(2)$ [fm] [23]. The lattice volume is 32^4 with periodic boundary conditions. We generate 4000 thermalized configurations. To improve a signal-to-noise ratio, the APE smearing technique is applied to the Wilson loop [24].

We measure all components of the Abelian electric fields $E_{Ai}(s) = \bar{\theta}_{4i}(s)$ and find that only E_{Az} is squeezed as shown in Fig. 3. We try to fit $\langle E_{Az}\rangle_W$ to a function $f(r) = c_1 \exp(-r/\lambda) + c_0$. Here λ corresponds to the penetration length. We obtain $\lambda = 0.128(2)$ [fm], which is similar to those obtained in the MA gauge and unitary gauges [11].

To see what squeezes the Abelian electric field, let us study the Abelian (dual) Ampère law

$$\vec{\nabla}\times\vec{E}_A = \partial_4 \vec{B}_A + 2\pi\vec{k}\,,$$

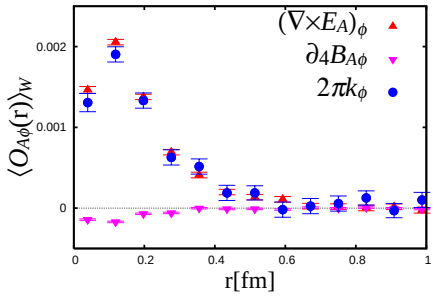

Figure 4: The curl of the Abelian electric field, magnetic displacement currents and monopole currents for $W(R=5a,T=5a)$.

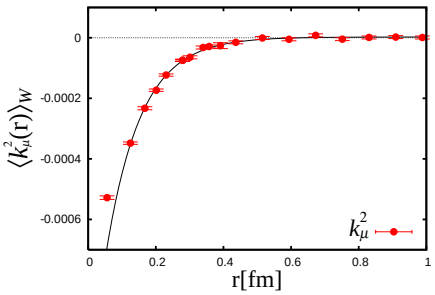

Figure 5: The correlation between the Wilson loop and the squared monopole density for $W(R=5a,T=5a)$. The solid line denotes the best exponential fit.

where $B_{Ai}(s)=(1/2)\varepsilon_{ijk}\bar{\theta}_{jk}(s)$. Each term is evaluated on the same mid-plane as for the electric field. We find that only the azimuthal components are non-vanishing, which are plotted in Fig. 4. Note that if the electric field is purely of the Coulomb type, the curl of electric field is zero. Contrary, the curl of the electric field is non-vanishing and is reproduced only by monopole currents. The magnetic displacement current is almost vanishing. These behaviors are clearly a signal of the Abelian dual Meissner effect, which are quite the same as those observed in the MA gauge [10].

5. Vacuum type

Fourthly, we may estimate the vacuum type by evaluating also the coherence length ξ from the correlation function between the Wilson loop and the squared monopole density $k_\mu^2(s)$ [25]. The correlation function is plotted in Fig. 5 and the coherence length extracted from the functional form $g(r)=c_1'\exp(-\sqrt{2}r/\xi)+c_0'$ is $\xi/\sqrt{2}=0.102(3)$ [fm]. The GL parameter $\sqrt{2}\kappa=\lambda/\xi=1.25(6)$ is close to the values obtained with gauge fixing[11]. Since the Wilson loop used here may still be small, what we can say is that the vacuum type is near the border between the type 1 and 2.

6. Confinement of non-Abelian color charge

The above results are quite remarkable in the sense that confinement of non-Abelian color charges can be explained in the framework of the Abelian dual Meissner effect. Since no gauge-fixing is done, gauge fields in any color direction are equivalent. Abelian electric fields in all color

directions are squeezed due to monopoles in the corresponding color direction. An Abelian neutral state in all color directions can survive as a physical state, and such a state is only the color singlet state. For example, consider meson states $u_c\bar{u_c}$ and $d_c\bar{d_c}$, where u_c (d_c) is an eigenstate of $\sigma_3/2$ with an eigenvalue $1/2$ $(-1/2)$. These are Abelian neutral in the $\sigma_3/2$ direction. Similarly, $U_c\bar{U_c}$ and $D_c\bar{D_c}$ are Abelian neutral in the $\sigma_1/2$ direction, where $U_c=(u_c+d_c)/\sqrt{2}$ $(D_c=(u_c-d_c)/\sqrt{2})$ is an eigenstate of $\sigma_1/2$. Note that $u_c\bar{u_c}$ $(U_c\bar{U_c})$ and $d_c\bar{d_c}$ $(D_c\bar{D_c})$ contain both Abelian charged and neutral states in the $\sigma_1/2$ $(\sigma_3/2)$ direction. But a SU(2) singlet state $u_c\bar{u_c}+d_c\bar{d_c}=U_c\bar{U_c}+D_c\bar{D_c}$ is Abelian neutral in all color directions. Hence confinement of non-Abelian color charge can be explained in terms of the Abelian confinement scenario of the dual Meissner effect.

References

[1] G. 't Hooft, in *Proceedings of the EPS International*, edited by A. Zichichi, p. 1225, 1976.

[2] S. Mandelstam, Phys. Rept. **23**, 245 (1976).

[3] G. 't Hooft, Nucl. Phys. **B190**, 455 (1981).

[4] Z. F. Ezawa and A. Iwazaki, Phys. Rev. **D25**, 2681 (1982).

[5] T. Suzuki, Prog. Theor. Phys. **80**, 929 (1988).

[6] S. Maedan and T. Suzuki, Prog. Theor. Phys. **81**, 229 (1989).

[7] T. Suzuki, Prog. Theor. Phys. **69**, 1827 (1983).

[8] A. S. Kronfeld, M. L. Laursen, G. Schierholz, and U. J. Wiese, Phys. Lett. **B198**, 516 (1987).

[9] T. Suzuki, Nucl. Phys. Proc. Suppl. **30**, 176 (1993).

[10] Y. Koma, M. Koma, E.-M. Ilgenfritz, and T. Suzuki, Phys. Rev. **D68**, 114504 (2003) and references therein.

[11] T. Sekido, K. Ishiguro, Y. Koma, Y. Mori, and T. Suzuki, Phys. Rev. **D76**, 031501 (2007).

[12] M. Lüscher and P. Weisz, JHEP **09**, 010 (2001).

[13] S. Necco and R. Sommer, Nucl. Phys. **B622**, 328 (2002).

[14] M. Lüscher and P. Weisz, JHEP **07**, 049 (2002).

[15] M. C. Ogilvie, Phys. Rev. **D59**, 074505 (1999).

[16] M. Faber, J. Greensite, and S. Olejnik, JHEP **01**, 008 (1999).

[17] T. Suzuki, S. Ilyar, Y. Matsubara, T. Okude, and K. Yotsuji, Phys. Lett. **B347**, 375 (1995).

[18] T. A. DeGrand and D. Toussaint, Phys. Rev. **D22**, 2478 (1980).

[19] A. Hasenfratz and F. Knechtli, Phys. Rev. **D64**, 034504 (2001).

[20] P. Cea and L. Cosmai, Phys. Rev. **D52**, 5152 (1995).

[21] A. Di Giacomo, M. Maggiore, and S. Olejnik, Phys. Lett. **B236**, 199 (1990).

[22] Y. Iwasaki, Nucl. Phys. **B258**, 141 (1985).

[23] T. Suzuki, K. Ishiguro, Y. Mori, and T. Sekido, Phys. Rev. Lett. **94**, 132001 (2005).

[24] APE, M. Albanese *et al.*, Phys. Lett. **B192**, 163 (1987).

[25] M. N. Chernodub *et al.*, Phys. Rev. **D72**, 074505 (2005).